


Article

## Prey fractionation in the Archaeocyatha and its implication for the ecology of the first animal reef systems

Jonathan B. Antcliff , William Jessop, and Allison C. Daley

**Abstract.**—Archaeocyaths are the most abundant sponges from the Cambrian period, having formed the first animal reef communities more than 500 million years ago. The Archaeocyatha are index fossils for correlating rocks of similar ages globally because of their abundance, extensive geographic distribution, detailed anatomy, and well-established taxonomy. Their ecological significance remains incompletely explored, yet they are known to have strongly competitively interacted, unlike modern sponges. This study examines the feeding ecology of the fossil remains of Siberian archaeocyath assemblages. As suspension feeders, archaeocyaths filtered plankton from the water column through pores in their outer wall. Here we outline a new method to estimate the limit on the upper size of plankton that could be consumed by an archaeocyath during life. The archaeocyaths examined were predominantly feeding on nanoplankton and microplankton such as phytoplankton and protozooplankton. Size-frequency distributions of pore sizes from six different Siberian archaeocyath assemblages, ranging from Tommotian to Botoman in age, reveal significantly different upper limits to the prey consumed at each locality. Some of the assemblages contain specimens that could have fed on larger organisms extending into the mesoplankton, including micro-invertebrates as a possible food resource. These results show that during the establishment of the first animal reef systems, prey partitioning was established as a way of reducing competition. This method has applicability for understanding the construction and the functioning of the first reef systems, as well as helping to understand modern reef systems and their development through time and space.

Jonathan B. Antcliff and Allison C. Daley. Oxford University Department of Zoology, South Parks Road, Oxford, U.K.; and Université de Lausanne, Institut des Sciences de la Terre, Bâtiment Géopolis, UNIL–Mouline, CH-1015 Lausanne, Switzerland. E-mail: [jonathan.antcliff@unil.ch](mailto:jonathan.antcliff@unil.ch), [Allison.daley@unil.ch](mailto:Allison.daley@unil.ch)

William Jessop. Oxford University Department of Zoology, South Parks Road, Oxford, U.K. E-mail: [will.m.jessop@gmail.com](mailto:will.m.jessop@gmail.com)

Accepted: 21 August 2019

First published online: 18 October 2019

Data available from the Dryad Digital Repository: <https://doi.org/10.5061/dryad.0r17c1m>

### Introduction

The Archaeocyatha are an extinct group of aspiculate sponges (Fig. 1) that appear very early in the Cambrian, forming extensive reef communities (Wood 1999; Debrenne 2007; Gandin and Debrenne 2010; Debrenne et al. 2012; R Core Team 2018) and shortly after the first appearance of sponge fossils (Carrera and Botting 2008; Antcliff 2013, 2015; Antcliff et al. 2014; Muscente et al. 2015; Nettersheim et al. 2019). While now widely recognized as an extinct class of Porifera (Debrenne et al. 2012; Antcliff et al. 2014), their taxonomic affinities were disputed until the 1990s (Debrenne and Vacelet 1984; Kruse 1990; Rowland 2001). Given their abundance and global distribution, the archaeocyaths have become important index fossils for correlating rocks on a

global scale, meaning that we have detailed knowledge of their taxonomy and systematics (Debrenne et al. 2012; Gradstein et al. 2012). The Archaeocyatha are the first undoubted metazoans to form extensive reef-like bioconstructions in association with calcimicrobes (Brasier 1976; Rowland and Gangloff 1988; Gandin and Debrenne 2010), and they therefore play a pivotal role in early Cambrian ecology (Wood et al. 1992; Wood 1999; Zhuravlev et al. 2015; Cordie and Dornbos 2019). Studies on their functional morphology have been extensive and show the Archaeocyatha were suspension feeders (Wood et al. 1992; Debrenne et al. 2012). The reef communities of archaeocyathan sponges meant many individuals lived in close proximity. Ordinarily such close assembly leads to increased

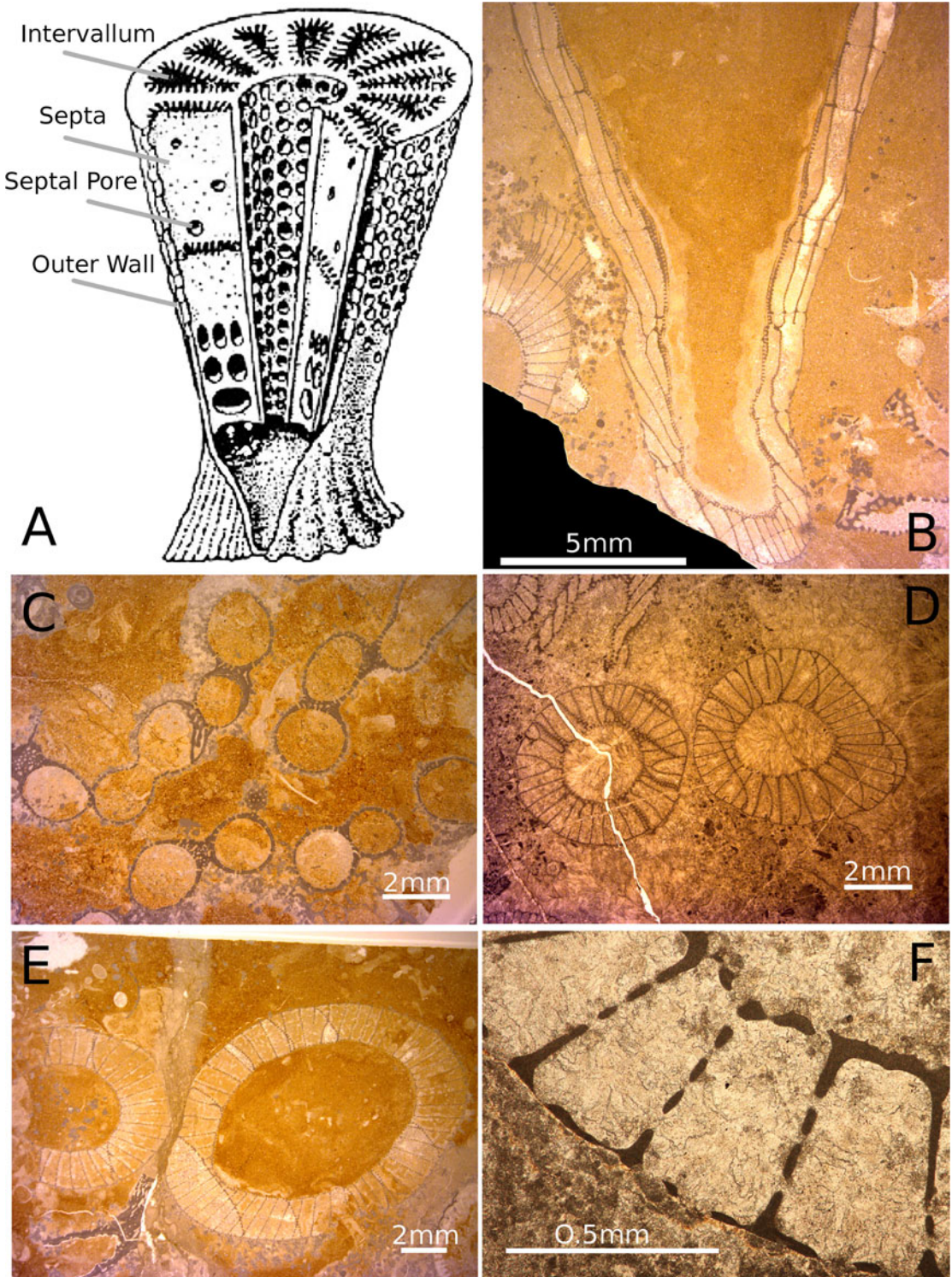


FIGURE 1. A, Schematic reconstruction of a double-walled archaeocyath showing the major characters discussed in the text. Adapted from a version in Antcliffe et al. (2014) from the original drawing of Debrenne et al. (1989). B–F, Archaeocyatha from the Siberian Platform in Russia, Terreneuvian to Cambrian Series 2 in age. B, A thin section of two archaeocyaths, central large specimen is in slightly oblique to longitudinal section, while the specimen in the bottom left is in transverse section. C, The archaeocyath *Archaeolynthus polaris* showing multiple modules. D, Two cups of an archaeocyath that show no growth avoidance and that are probably conspecific. E, Two cups of different archaeocyathan individuals showing growth avoidance. F, Close-up view of the two-walled structure of an archaeocyath showing the inner and outer walls, the septa, the intervallum space, and the inner-wall pores, outer-wall pores, and septal pores.



competition for suspended food resources, particularly given that in the early Cambrian the global abundance of phytoplankton and zooplankton is thought to have been much lower than modern levels (Servais et al. 2010; Cordie et al. 2019). In modern animal communities, resource partitioning is a common strategy used to reduce food competition between coexisting taxa (Gili and Coma 1998). However, it has long been known that modern sponge communities do not play by the same ecological rules as most metazoan communities (Reiswig 1971; Wulff 2006). Modern sponges do not partition prey before ingestion, only during retention, meaning there is little competition between them for this resource (Reiswig 1971). As a result, sponge-dominated communities are almost invariably not competition driven, but neutral associations (Reiswig 1973). It seems that modern sponges are “different from all the other organisms for which the conceptual framework of ecology was developed” (Wulff 2006: p. 148). Sponge interactions, particularly in modern sponge-dominated communities, generally promote the “continued coexistence of all participating species” (Wulff 2012: p. 274). Such cooperation and passive association have not been observed for many Cambrian sponge communities formed by archaeocyaths (Zhuravlev et al. 2015). Rather, competitive interactions are well documented in Archaeocyaths, including characteristics such as overgrowth (bioimmuration), avoidance, and the secretion of aporous skeletal sheets to maintain barriers between individuals (Brasier 1976; Kruse 1990; Debrenne et al. 2012). Statistical analysis of extensive ecological data sets also indicate that archaeocyathan communities were selectively assembled (Zhuravlev et al. 2015), meaning that the individuals were competing to be present in the community. Archaeocyathan communities therefore behaved rather differently compared with modern sponge-dominated communities, and this seems to have been particularly true during the Tommotian (Cambrian Stage 2 in Siberia, Russia).

The structure of an archaeocyath skeleton (Fig. 1A,B) is thought to reflect the organization of the aquiferous system in life (Wood et al. 1992). As suspension feeders, archaeocyaths

filtered organic matter from the water column, which they brought into their body through pores or canals in their skeleton (Debrenne et al. 2012). Archaeocyaths had choanocytes (Debrenne et al. 2012) that would have helped generate a current drawing water from the outside of the sponge through the outer wall into the intervallum, the space between the inner and outer walls, and then out of the inner-wall pores to where it would have exited the cup (Balsam and Vogel 1973). While some archaeocyaths were single walled (e.g., *Archaeolynthus*; Fig. 1C) most archaeocyaths had double walls (Fig. 1A,D–F), and the majority of living matter was located in the intervallum (the space between the two walls), and it would be here that phagocytosis of food would have taken place (Savarese 1992; Debrenne et al. 2012). The morphology of archaeocyaths is radically different from that of any living sponges, with the single genus *Vaceletia* being the only approximate morphological analogue, as the only surviving sphinctozoan sponge (Vacelet 1977; Wörheide and Reitner 1996). Sphinctozoans are a polyphyletic grouping of similarly constructed sponges that reached their peak during the Permo-Triassic (Senowbari-Daryan and García-Bellido 2002). There are many similarities between the polyphyletic sphinctozoan sponges and archaeocyaths, including the lack of spicules (e.g., in *Vaceletia*; see Vacelet 1977), the massive calcareous skeleton, and the segmentation and partitioning of the skeleton (Kruse 1990). However, there are also fundamental differences such as the wall/pore elaborations in archaeocyaths, which are entirely absent in sphinctozoans. The wall microstructure is also different between archaeocyaths and sphinctozoan sponges, as is the stereoplasm, and the ontogenetic sequence of wall production, particularly in relation to the intervallum where food digestion takes place (Kruse 1990). Archaeocyaths are therefore unique in the evolutionary history of sponges and are morphologically distinct from all living sponges.

There has been little examination of what characters of the archaeocyaths were the primary focus for the observed competitive exclusions. According to ecology theory, the primary driving factors of competition are: resources (primarily food), the natural

environment (e.g., space), and natural enemies (e.g., predators; Shea and Chesson 2002). As archaeocyaths had no known natural predators, and ecological studies suggest that they were often pioneer species so had little competition for local space (Zhuravlev et al. 2015), we here test the hypothesis that food was a limiting resource that drove competition in archaeocyathan communities. What archaeocyaths fed on is unknown, but is usually assumed to be bacteria, as these are important to the diet of extant sponges (Kruse et al. 1995; Debrenne and Zhuravlev 1997). Modern sponges can feed on the whole size range of particles that can enter through their pores (ostia), albeit generally with reduced efficiency with increasing particle size (Leys and Eerkes-Medrano 2006). In archaeocyathan sponges, the size of the pores on the outer wall logically limited the size of food particles entering the skeleton, and when measured consistently, pore size can therefore provide an upper bound on the size of plankton that could have been phagocytosed by internal feeding cells. Archaeocyath outer-wall pore sizes, as well as septal and inner-wall pores (Fig. 1A,F), have been measured as a taxonomic indicator (Kruse 1982; Skorlotova 2013; Kruse and Moreno-Eiris 2014); however, pores have never been examined in an ecological context. Here we describe the feeding dynamics and prey partitioning of archaeocyathan reef communities by using measurements of the outer-wall pore diameter as a proxy for delimiting the size of suspended plankton entering the body and being consumed by the animal. Restrictive pore size data can also be used to examine the type of prey being consumed, because plankton fall broadly into distinct size categories that correlate well with biological grouping (Sieburth et al. 1978).

### Materials and Methods

The archaeocyath material studied was derived from localities on the Siberian Platform in Russia (Fig. 2A) and is housed in the collections at the Muséum National d'Histoire Naturelle (MNHN) in Paris, France. The Siberian Platform consists of three major facies tracts of lower Cambrian, Nemakit–Daldynian to

Toyonian in age, equivalent to Cambrian Series 1 (Terreneuvian) and Series 2, which displaced northeastward throughout the Cambrian (Khomentovskiy and Repina 1965). The fossil localities are now found where the Lena and Aldan Rivers intersect the archaeocyathan reef system. In general, there is a SW–NE trend of increasing paleo-water depth (Fig. 2A,B), with the archaeocyathan reef acting as a barrier between the shallow-marine, evaporitic, terrigenous system to the SW and the open fully marine deeper-water carbonates to the NE (Kruse et al. 1995). The specimens were predominantly collected during fieldwork by Peter D. Kruse, Andrey Yu. Zhuravlev, and Noel P. James (Kruse et al. 1995), from six localities in Siberia: Aldan, Byd'yangaya Creek, Churan, Zhurinskiy Mys', Titirikteekh, and Oy-Muran (Fig. 2C). Archaeocyaths at these localities form meter-scale bioherms, where calcimicrobes such as *Renalcis*, living in association with the archaeocyaths were responsible for precipitating the majority of the calcium carbonate that comprises the bioherms (James and Debrenne 1980; Gandin and Debrenne 2010). Taxa included in this study include the genera *Nochoroicyathus*, *Coscinoicyathus*, *Rotundocyathus*, *Erismacoscinus*, and *Tumuliolythnus* (Fig. 3).

The global correlations of Cambrian strata are notoriously problematic, with only a few sections in the world (mainly Gondwana, e.g., Morocco and Australia, and Avalonia, e.g., the United Kingdom and Canada) providing any (even if very limited) absolute dates (Landing et al. 2013). The difficulties are then compounded by major facies differences between the different global sections, leading to extreme endemism of the fossils and making global biostratigraphy problematic and contentious (Landing et al. 2013). Most stratigraphic sections contain no lower Cambrian rocks (Peters and Gaines 2012). This time period coincided with one of the largest marine transgressions in Earth history, leading to subsequent extensive erosion and loss of lower Cambrian rock (Peters and Gaines 2012) as sea levels receded. As a result, lower Cambrian rocks are rare and difficult to correlate. Figure 2D compares the locally used stratigraphic terminology for Siberia with that of the globally correlated IGCP (International Geoscience Programme) series and

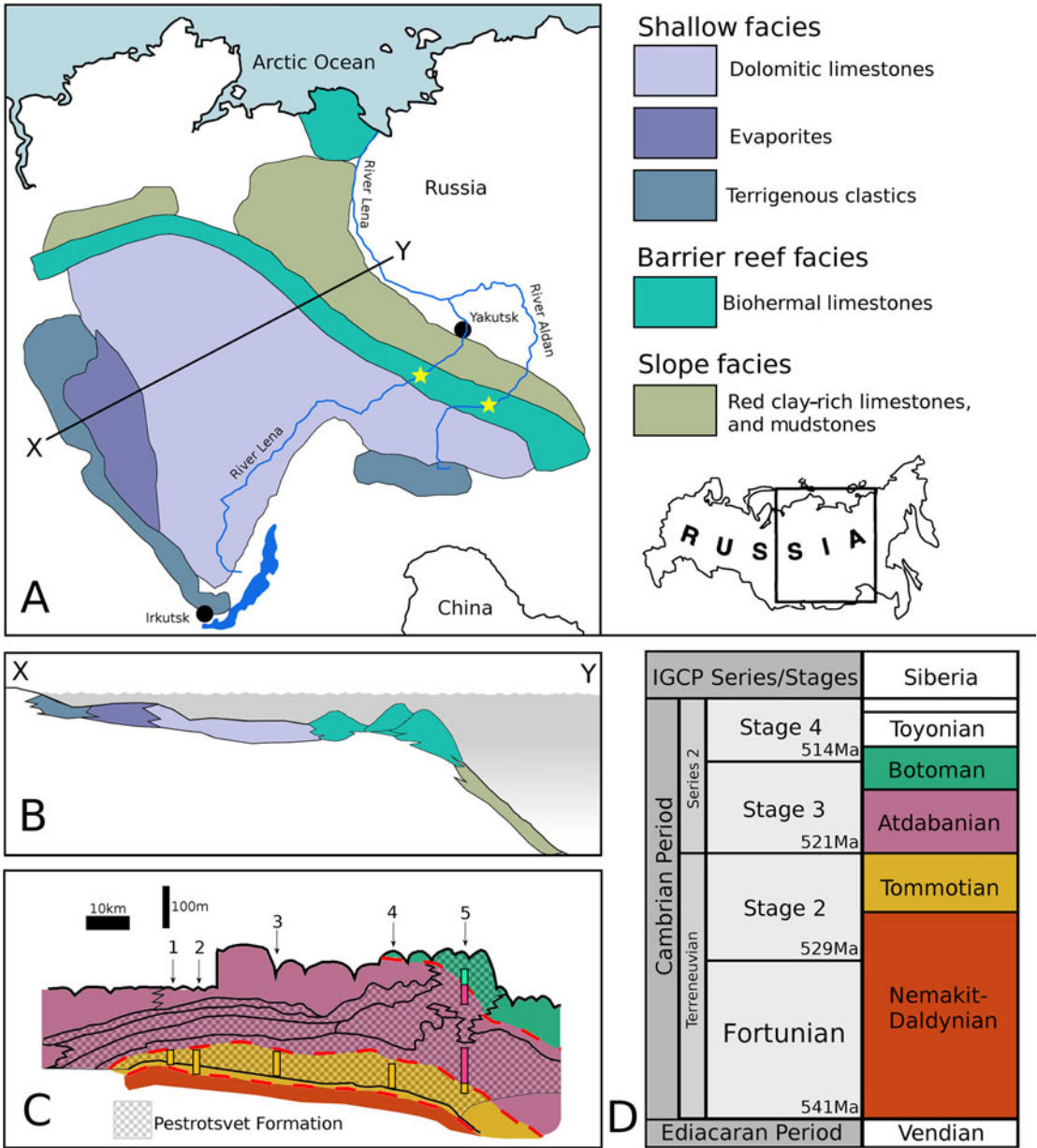


FIGURE 2. A, Map of the locality of the Siberian Platform in Russia, showing the extent of the platform with the three major facies tracts of Terreneuvian to Cambrian Series 2 in age. Stars show the position of the fossil localities on the Lena and Aldan Rivers from which the samples used in this study were taken. In general, there is a SW–NE trend of increasing paleo-water depth, with the archaeocyathan reef acting as a barrier between the shallow restricted marine system to the SW and the deeper marine system to the NE. Line X–Y denotes the line of section in part B. B, Schematic reconstruction of the facies relationships of the Siberian Cambrian. C, Schematic of a section along the River Lena, with the Pestrotsvet Formation crosshatched. Shadings (colors online) correspond to the timescale in D. Numbers indicate the positions of the localities discussed: 1. Titirikteekh; 2. Churan; 3. Byd’yangaya; 4. Zhurinskiy Mys; 5. Oy-Muran. Highlighted bars show what age the specimens were drawn from for a particular section. After Kruse et al. (1995). D, Timescale showing current best estimates for how the Siberian sections correlate with the global stage and series boundaries as recognized by the IGCP (Cambrian), compiled from Kruse et al. (1995), Rozanov et al. (2008), Gradstein et al. (2012), and Landing et al. (2013).



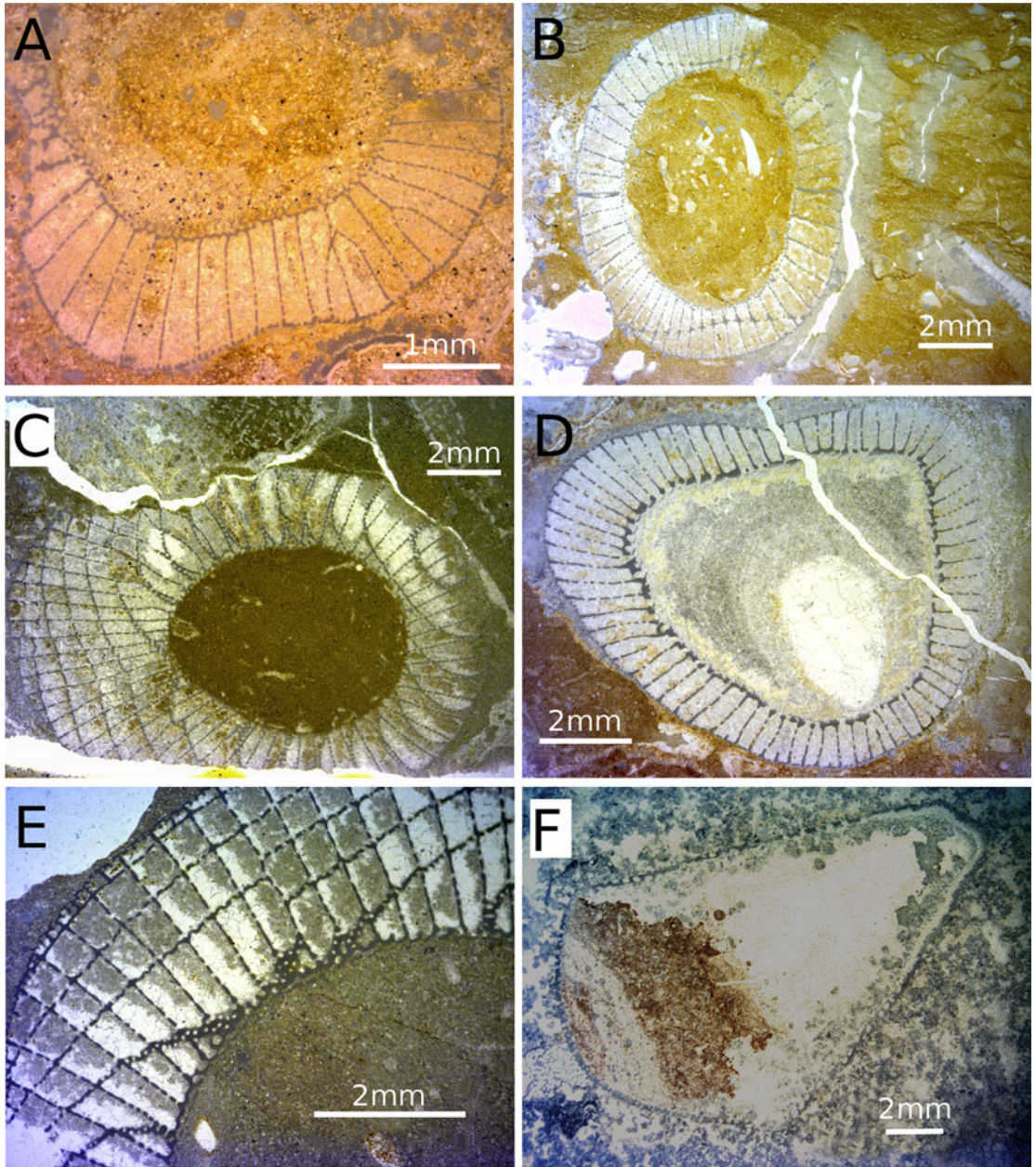


FIGURE 3. Representative genera of Archaeocyatha from the Siberian fossil sites around the Lena River. All are from the collections in the Muséum National d'Histoire Naturelle in Paris. A,B, *Nochorocyathus*; C, *Coscinocyathus*; D, *Rotundocyathus*; E, *Erimacoscinus*; F, *Tumuliolythus*.

stages. As these correlations remain to some extent problematic (Rožanov et al. 2008; Landing et al. 2013; Daley et al. 2018), the internally consistent Siberian terminology is adopted here, as that is how the material was catalogued in MNHN based on previous descriptions and the fieldwork collection data (Kruse et al. 1995).

The Oy-Muran material is difficult to date and was collected from two areas of distinct ages within the locality (Fig. 2). Consequently, they are separated in the analysis according to age: one is of latest Tommotian to Atdabanian (referred to as To-At Oy-Muran) and the other is dated between the Atdabanian and Botoman

(At-Bo Oy-Muran). All the other localities are Tommotian in age. Within the Tommotian, Aldan is from the oldest strata; Churan, Titirik-teekh, and Zhurinskiy Mys' are all three derived from strata of a slightly younger age; and Byd'yangaya Creek is from the youngest strata (Kruse et al. 1995). They were also separated spatially, with each locality representing an area of exposed strata spaced several kilometers apart (Kruse et al. 1995) along the River Lena, while Aldan comes from sections on the River Aldan. (Fig. 2A,C).

Measurements of archaeocyaths were taken from rock thin sections mounted on glass slides. Any individual archaeocyath is referred to as a specimen, such that there may be multiple specimens on each thin section. The specimens from which measurements could be taken were identified to a genus level on each thin section by previous researchers, and when unclear, they were identified with help from A. Kerner (MNHN). A specimen was identified as suitable for use if it was possible to take at least five representative outer-wall pore measurements, although usually around 10 measurements were taken from each specimen. Pores had to be well enough preserved that the area within and around a pore could be distinguished clearly. Each thin section examined was digitally scanned, and the specimens to be measured were assigned labels (Supplementary Material). A Heidenhain Quadra-Chek with a Nikon Measuring Microscope with a binocular head was used to take the measurements.

Archaeocyaths can be clonally modular, that is, constructed of more than one cup (Debrenne et al. 2012) and are one of the earliest animal groups to have become clonal (Landing et al. 2018). In life, the archaeocyath would have branched when creating clonal modules, which in thin section is not immediately obvious, because the connection may not be visible in the plane of section. Thus, one individual might produce many cups, which could appear to be separate individuals in thin section. This could lead to pore sizes on cups from the same individual being counted twice as separate specimens. It is therefore necessary to be able to distinguish between cups of separate individuals in close proximity and cups of

one modular individual (Fig. 1C–E). Several indicators were used to distinguish modular forms from separate individuals, including the presence of immune responses (Brasier 1976) to dismiss the possibility of two or more morphologically similar archaeocyaths in close proximity being one modular form. Most of the archaeocyath species examined in this study were not modular, as modularity was rare in the Tommotian (Wood et al. 1992).

Two different procedures were developed for measuring restrictive pore size depending on whether the section through the pore was transverse or longitudinal (Fig. 4). If a pore was cut at an angle that departed from either the longitudinal cut or the transverse cut, measurements were not taken, as neither technique would be appropriate (Figs. 4 and 5A,B). This often meant entire specimens were rejected, as all the pores were oblique cuts. To ensure the accuracy of the measurement from the information that can be gained from one view, each specimen was compared with different cuts of congeneric specimens. Previous studies measured outer-wall pore sizes (Kruse 1982; Skorlotova 2013; Kruse and Moreno-Eiris 2014) but did not take into account the commonly present features of pores that would have restricted the size of plankton that could pass through those pores. Such features include bracts (Fig. 5C), tumuli (Fig. 5D), and microporous sheaths. All of these features would have limited the size of particles that could pass into the archaeocyath. When such structures were present in the studied material, measurements were taken of the unobstructed gap left open by the additional feature. Broken walls were disregarded so as not to overestimate pore sizes (Fig. 5E). When both types of view were available on the same specimen, measurements were taken from both for later comparison (Fig. 5F). Having both longitudinal and transverse sections provides a complementary view of the pores to gain maximum information about the shape and structure of the pore.

#### Measuring Outer-Wall Pore Diameter in Transverse View

A transverse view of an archaeocyath pore intersects the pore in a plane perpendicular to the surface of the outer wall. In thin section,



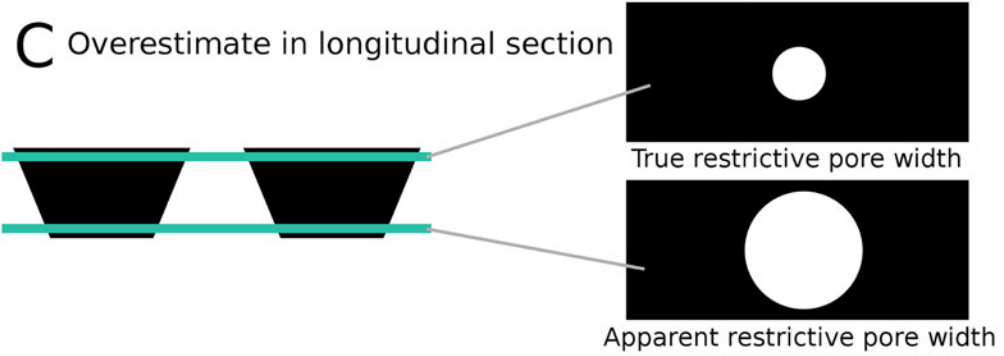
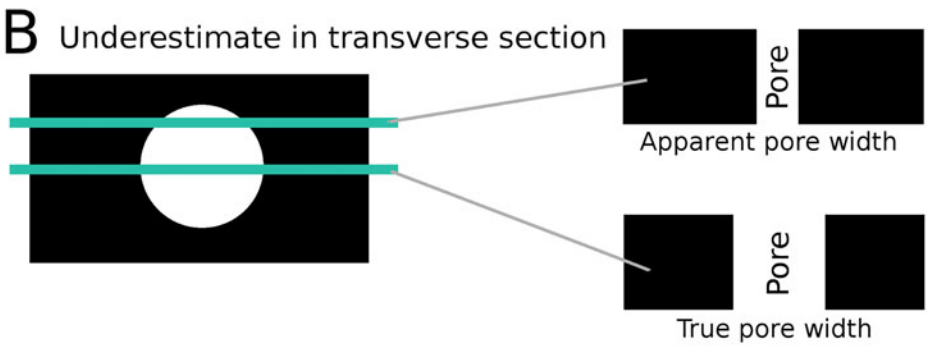
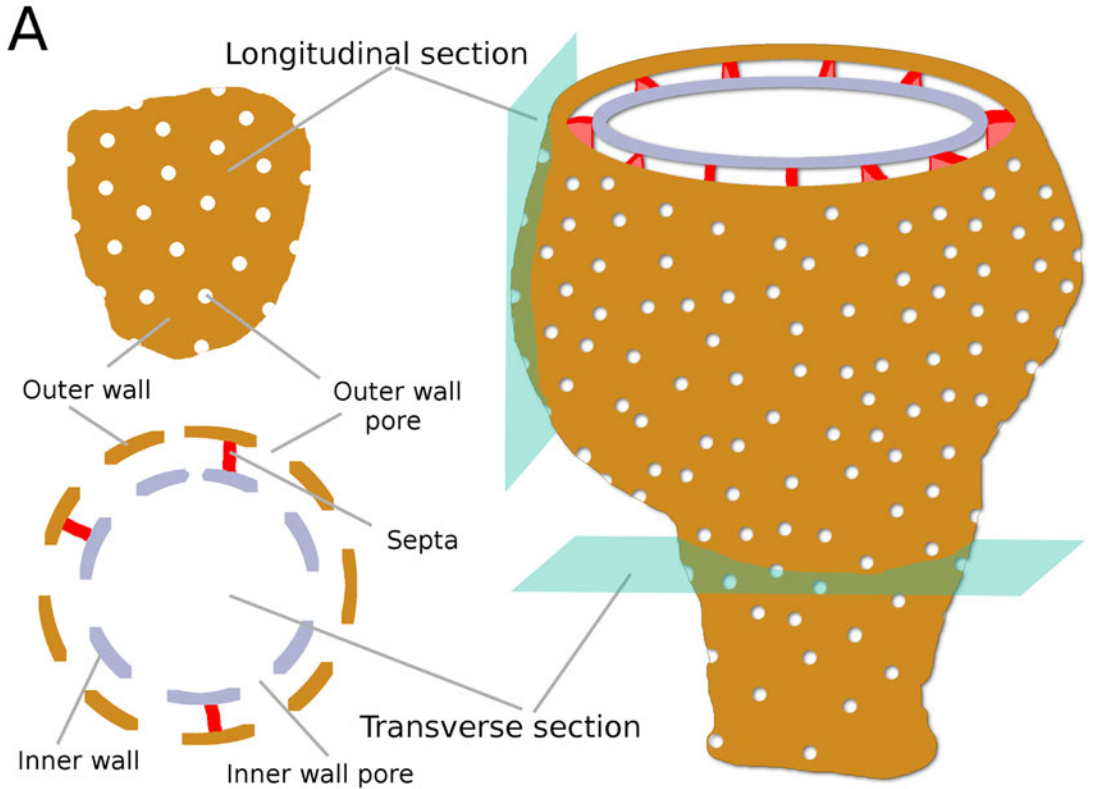


FIGURE 4. A, Schematic reconstruction of a typical archaeocyath showing the relationship of the major anatomical features to both longitudinal and transverse sections. B, Schematic drawing showing how pores in transverse section could appear smaller than the true diameter, if the section passes through anywhere other than the exact center of the pore. C, Schematic showing how pores in longitudinal view could appear larger than the true restrictive width, depending on the location of the section.



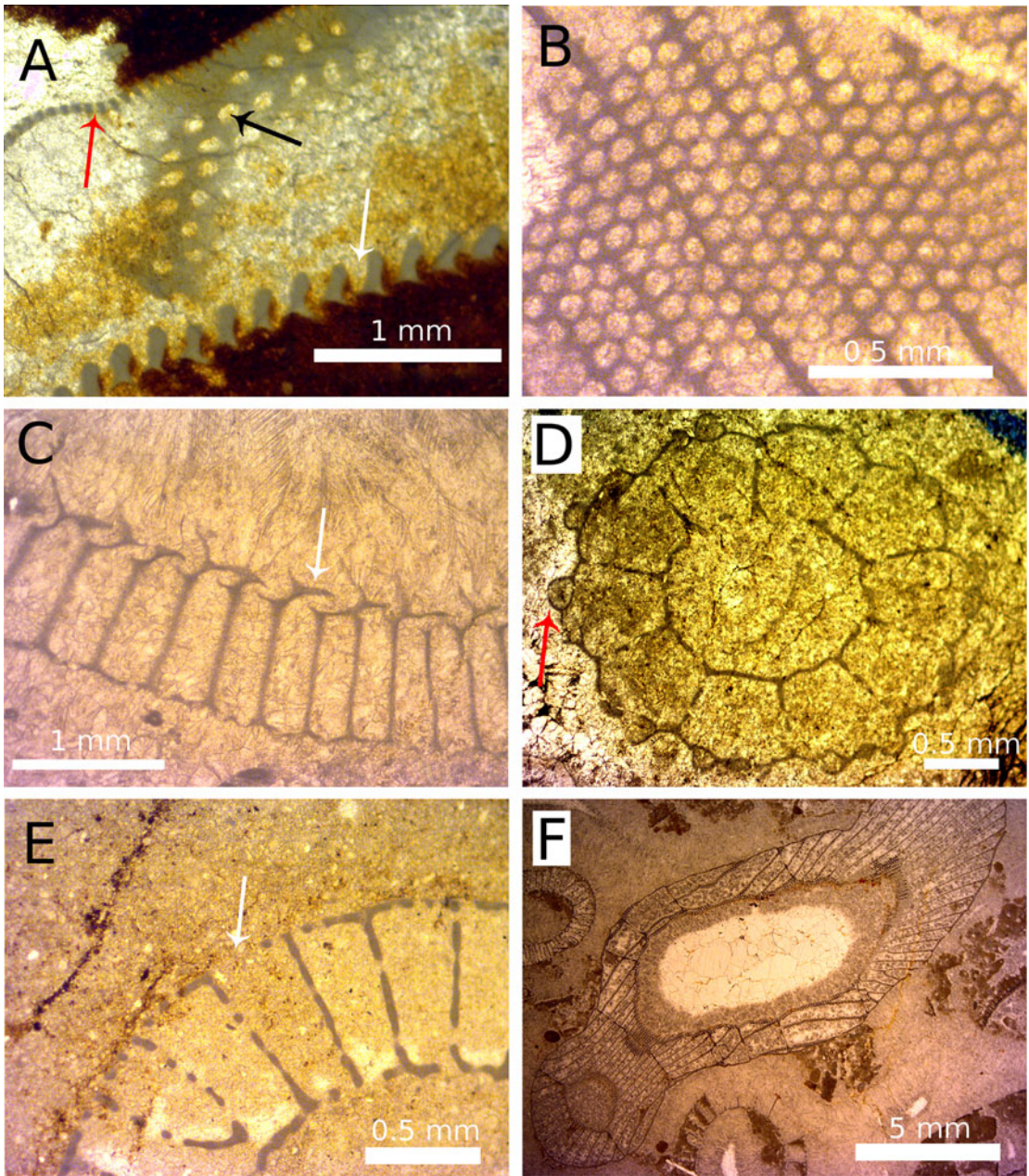


FIGURE 5. A range of features associated with pores and apparent restrictive pore widths. A, the three major pore types: dark gray (red online) arrow, outer-wall pore; black arrow, septal pore; white arrow, inner-wall canal. B, Varying pore sizes seen in slightly oblique section, with pores becoming more elliptical (to subpolygonal) to the right side of the image. C, Annuli are plate-like features (white arrow) that restrict the pore width and may add spiny and ornate coverings to the pore. D, Tumuli are sphere-like coverings (dark gray [red online] arrow) over pores that have one or more openings to allow transit of particles. E, An example of a broken outer wall (white arrow), producing a space in the wall much larger than the original pore. F, The irregular growth of archaeocyaths (e.g., if the specimens turns through 90° during growth) means that a single section can intersect the specimen in such a way that transverse, oblique, and longitudinal sections can be seen in a single specimen in thin section.

pores in transverse view are visible along their entire depth from the exterior surface to the interior surface of the outer wall (Fig. 4C, right). In some specimens, the pore is parallel sided; alternatively, the pore diameter can narrow (be funnel shaped) along its length (Debrenne et al. 2012). In the case of a funnel-shaped pore, the restrictive pore size is the narrowest end of the pore. A transverse cut through a pore might make pore size appear smaller than it actually is if the cross-section does not cut through the pore at its maximum width (Fig. 4B, top right). Thus, thin sections of archaeocyaths can be misleading (McKee 1963). To resolve this problem, measurements of restrictive pore size were only taken from the apparently largest pores on a specimen, as is the convention used by studies that measure other aspects of pore sizes (Kruse 1982; Skorlotova 2013; Kruse and Moreno-Eiris 2014). So in transverse view, restrictive pore size comes from the largest pores visible in section.

#### Measuring Outer-Wall Pore Diameter in Longitudinal View

Longitudinal views of pores intersect pores in a plane parallel to the outer-wall surface, such that the pores appear as circles in thin section. Incidentally, a longitudinal view of a pore will usually intersect the archaeocyathan cup slightly obliquely as the tangent to the cup wall, so a longitudinal cup view and a longitudinal pore view do not have to be the same, unless the wall is parallel to the cup axis. Longitudinal pore views only show the diameter of the pore at one point along its whole depth, and it can be unclear whether this is the narrowest point, potentially leading to overestimation of the restrictive pore size (Fig. 4C, right). To resolve this, only the pores that appeared smallest were measured. This approach also resolved problems connected to the presence of any features associated with more complex pores. For example, if the pores had bracts, the gap between the bract and the pore wall (the restrictive pore size) would appear smallest on the thin section. A few species of archaeocyaths have two distinct pore sizes, with one being noticeably smaller than the other. In these instances, the smallest pores among the distinctly bigger pores were

measured. It should be noted that specimens with two distinct pore sizes would not affect the transverse view method, as the smaller pore type would be treated as an artifact and dismissed, because the largest visible pore diameter is measured in transverse view. Longitudinal views of pores often appeared noncircular. There are two reasons for this. First, if circular pores were cut at a slightly oblique angle, then pores would appear oval shaped (McKee 1963). This is an artifact, and the true restrictive diameter can still be measured from the shortest dimension. Second, some archaeocyath species have true noncircular pores, although this was the case for only one taxon measured in this study. For noncircular pores, only the shortest distance was measured (the minor axis of the ellipse), as ingestion was still limited by the shortest distance across the pore.

#### Analyses

Data collected were input into Microsoft Office Excel and used to calculate mean outer-wall pore size, standard deviation, and coefficient of variance for each specimen. The statistical program R (R Core Team 2018) was used, specifically the packages *arm* for correlation and regression analyses and *ggplot2* for plotting the figures. PAST (Hammer and Harper 2008) was used for Kolmogorov-Smirnov tests for examining data distribution. Pearson's was used for all correlations unless otherwise stated. All results are reported as three significant figures, unless an exact result was obtained. The results are split into four parts, the first two of which aim to test the validity of the methods. The second two aim to investigate aspects of archaeocyath feeding ecology. The method of analysis for each of these categories is described in the following sections.

#### Analyses of Transverse and Longitudinal Measurements from the Same Specimens

The aim of these tests was to determine whether the method used on longitudinal pores was measuring the same diameter as the method used to measure transverse pores. All the data for specimens across all the localities for which both longitudinal and transverse



measurements had been taken were compiled, and mean pore sizes of each specimen were calculated for pores measured from the transverse and longitudinal sections separately. The two mean pore sizes were examined with linear regression, with a paired *t*-test performed for the support of regression gradient. The null hypothesis of these tests is that there are no significant differences between the mean pore sizes measured from transverse and longitudinal sections. As neither the transverse nor the longitudinal measurements can be designated as the dependent or independent variable, two linear regressions were carried out (*x* on *y* and *y* on *x*). One was for the transverse measurement against the longitudinal measurements. This makes transverse measurements the dependent variable, and so all the error is attributed to the transverse measurements. The other regression made longitudinal measurements the dependent variable so that the situation was reversed. The standard deviations and coefficients of variance of the measurements were also compared between the transverse and longitudinal data sets using *t*-tests and linear correlation to compare the dispersion of the measurements. The aim of these tests was to investigate whether there was equal variability in the longitudinal and transverse measurements from each individual specimen.

#### Analyses of Transverse and Longitudinal Measurements when Only One Type of Outer-Wall Pore View Was Taken per Specimen

Mean pore size data were collated for specimens in which pores in only one view had been measured. Although all the mean pore sizes of transverse measurements had been taken from different specimens than were used for the longitudinal measurements, it was reasoned that, for a locality, the transverse and longitudinal measurements should not be significantly different from each other, because the specimens for both theoretically represent a random sample of the same population. For this reason, the transverse and longitudinal measurements were only compared if they were from the same locality. Any significant differences in the overall mean of the mean pore sizes of transverse versus longitudinal

measurements were tested using a Welch's *t*-test. A Welch's *t*-test was used as there would otherwise have been a slight violation in the assumption of constant variance. Data were subjected to a Box-Cox transformation to improve normality. These tests were used to investigate whether the mean pore size distribution for a locality as calculated from specimens for which only transverse measurements were taken was significantly different from the pore size distributions calculated from specimens from which only longitudinal measurements had been taken.

#### Comparisons of the Distribution of Mean Outer-Wall Pore Sizes between Localities

The aim of these tests was to test for any significant differences between the distribution of pore sizes found at the different localities. Comparisons were made of the distribution of pore sizes at each locality using a series of two-sample Kolmogorov-Smirnov tests, a test that does not make any assumptions about the distribution of the data. This test compares the overall distribution of two samples by comparing the maximum difference between their cumulative probability distributions (Hammer and Harper 2008). The test was carried out on every combination of localities. As 21 tests had been carried out in total, the Benjamini-Hochberg procedure was used to control the false discovery rate, for a false discovery rate of 5%.

## Results

#### Analyses of Transverse and Longitudinal Measurements from the Same Specimens

*Comparisons of the Mean Outer-Wall Pore Sizes.*—In total there were 76 specimens for which mean pore size was calculated using both transverse and longitudinal measurements. A two-tailed paired *t*-test between the overall mean pore sizes of the longitudinal and transverse measurements showed no significant difference ( $t(75) = 0.46$ ,  $p$ -value = 0.640). This provides evidence that there is no systematic difference between the two methods. Results of the linear correlation analyses indicate that there is a highly significant correlation between the size of pores as measured by



TABLE 1. The 95% confidence intervals for two linear regression analyses comparing outer-wall pore diameter measured from longitudinal and transverse sections.

	Confidence intervals of transverse on longitudinal		Confidence intervals of longitudinal on transverse	
	2.5%	97.5%	2.5%	97.5%
Confidence interval	2.5%	97.5%	2.5%	97.5%
Intercept	-3.73	5.43	-0.51	8.31
Slope	0.92	1.04	0.89	1.01

transverse and longitudinal mean pore size ( $r^2 = 0.930$ ,  $F(1,74) = 946$ ,  $p$ -value  $< 2.20 \times 10^{-16}$ ).

An analysis of the correlation between transverse and longitudinal measurements was performed when these could be measured from the same specimen. The regression of longitudinal mean pore size on transverse mean pore size gave a slope of 0.95 and an intercept of 3.90. The regression of transverse mean pore size on longitudinal mean pore size gave a slope of 0.98 and an intercept of 0.85. The 95% confidence intervals (Table 1) for both regressions show that the intercept is not significantly different from 0 and the slope is not significantly different from 1 at the 95% confidence level, providing evidence that the two methods are measuring the same diameter. The lower bound for the gradient of the slope is 0.96 and the upper is 1.09, which still contains a slope of 1 (Fig. 6). The true relationship between the mean pore sizes as calculated by the two types of measurement would be expected to lie between these two lines with allowance for the small uncertainty of their confidence intervals. The correlation for longitudinal on transverse is excellent ( $r^2 = 0.938$ ) and highly significant ( $p$ -value [slope] =  $1.00 \times 10^{-45}$ ). The results of these tests provide good evidence that the two types of measurement are measuring the same average pore diameter.

*Comparisons of Standard Deviation and Coefficient of Variance of Measurements used to Calculate Mean Outer-Wall Pore Size.*—The standard deviation was calculated for the measurements used to calculate mean pore size; there was a sample size of 70 SDs for transverse and longitudinal measurements. The two-tailed paired  $t$ -test gave an insignificant result ( $t(69) = 0.0441$ ,  $p = 0.964$ ). This indicates that the overall mean standard deviation for the transverse

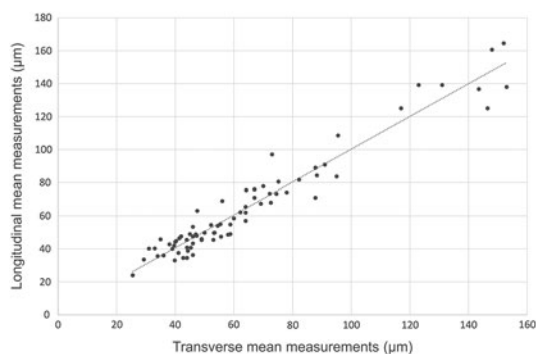


FIGURE 6. Plot showing the correlation between outer-wall pore measurements in transverse and longitudinal section ( $n = 257$  specimens).

measurements is not significantly different from that of the longitudinal measurements. The correlation coefficient for the two variables was 0.570 ( $p$ -value =  $1.97 \times 10^{-7}$ ). This highly significant correlation suggests that the standard deviation of both transverse and longitudinal measurements increases as the other increases. To test this, the coefficient of variance was calculated for all the measurements for which standard deviation had been calculated. There was no correlation between the coefficient of variance for the transverse versus the longitudinal measurements ( $r^2 = 0.140$ ,  $p$ -value = 0.235). These results support the hypothesis that the correlation in standard deviations was caused by the increase in mean pore size. Further, a paired  $t$ -test for the coefficient of variance also found no significant difference between the mean of the coefficient of variances for the two methods ( $t(69) = 0.345$ ,  $p$ -value = 0.731). So neither method had a consistently higher coefficient of variance.

#### Transverse and Longitudinal Measurements when Only One Type of Outer-Wall Pore View Was Taken per Specimen

Box plots of the data (Fig. 7) show a trend of longitudinal measurements having lower medians and upper-quartile and lower-quartile values than transverse measurements. The longitudinal measurements also have a smaller interquartile range. Statistical tests were only carried out for data from At-Bo Oy-Muran and To-At Oy-Muran, because these sites had reasonably large and even sample sizes (26

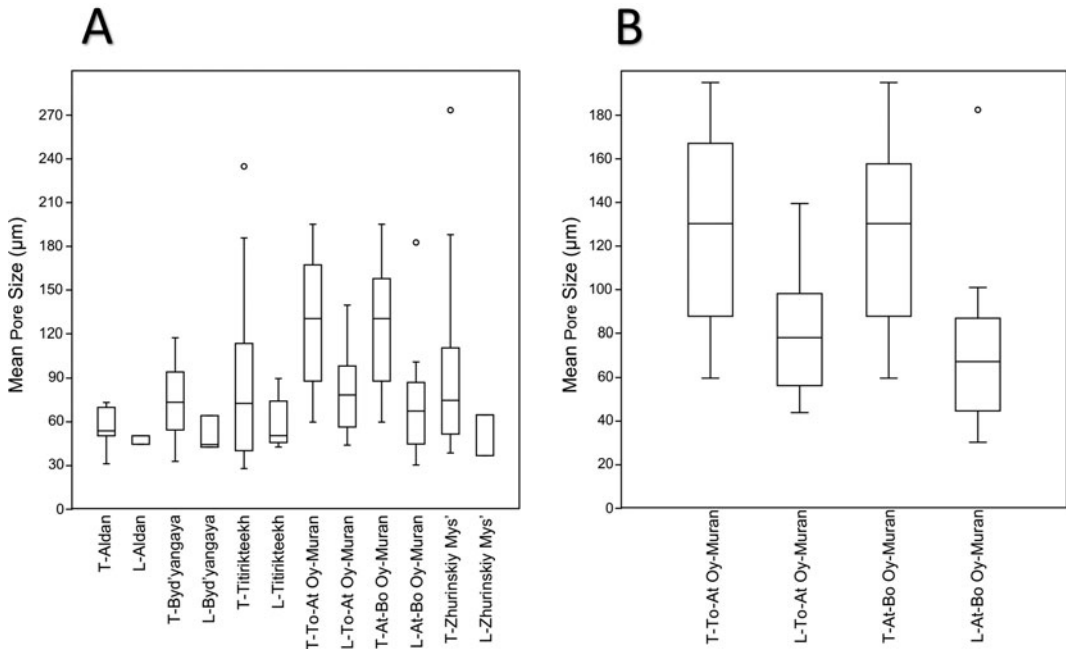


FIGURE 7. Box plots of outer-wall pore sizes measured separately for locality and section orientation. Any locality names with the prefix “T” are measurements from transverse sections, and those localities with prefix “L” are measurements from longitudinal sections. The horizontal lines in the boxes represent, in order from top to bottom, the upper quartile, the median, and the lower quartile. Whiskers show the minimum and maximum values, excluding outliers. Outliers were defined as being further than 1.5 times the height of the box away from the box and are signified by circles. A, Data from all locality studies. B, Enlarged box plots for the two Oy-Muran localities.

for To-At Oy-Muran and 31 for At-Bo Oy-Muran; Fig. 7B). Welch’s two-tailed *t*-tests were used on the transformed data for To-At Oy-Muran and At-Bo Oy-Muran. The result of the *t*-tests showed the means of the two types of measurements were significantly different from each other ( $t(23.2) = 3.0491$ ,  $p$ -value = 0.00576 for To-At Oy-Muran and  $t(28.8) = 4.00$ ,  $p$ -value = 0.000400 for At-Bo Oy-Muran). The 95% confidence intervals for the differences between the means showed that the mean longitudinal pore size ( $\mu L$ ) was significantly less than the mean transverse pore size ( $\mu T$ ) for both localities ( $-2.22 < \mu L - \mu T < -0.42$  for To-At Oy-Muran;  $-2.61 < \mu L - \mu T < -0.85$ ).

#### Summary Statistics of the Mean Outer-Wall Pore Sizes

In total, data were collected for 257 specimens. The mean pore size for all the localities’ data combined was 81.5  $\mu\text{m}$ , and the median pore size was 68.8  $\mu\text{m}$ . The data were positively skewed, so although the maximum pore size

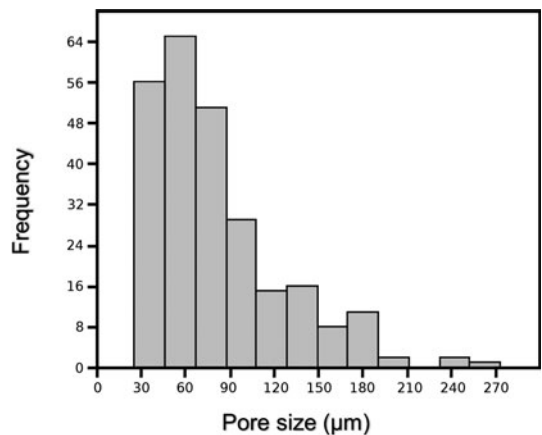


FIGURE 8. Histogram showing the frequency of archaeocyath specimens with a mean outer-wall pore size falling within the given size classes (12 bars, 21  $\mu\text{m}$  wide). The global median is 68.8  $\mu\text{m}$  and the global mean is 81.5  $\mu\text{m}$ . The data skew positive, with 75% of specimens having pores smaller than 101  $\mu\text{m}$ . The smallest mean restrictive pore size found was 25  $\mu\text{m}$ , while the largest was 273  $\mu\text{m}$ .

was 273  $\mu\text{m}$ , there were proportionally fewer high values with 75% of the data below 101  $\mu\text{m}$  (Fig. 8). The minimum size recorded was 25.2  $\mu\text{m}$ .

TABLE 2. Comparing the outer-wall pore distributions by locality. The *p*-values for each pair of localities are shown above the diagonal line of black boxes, with bold text indicating significant results at 95% confidence after the Benjamini-Hochberg procedure. Below the line are the *D*-values associated with the *p*-values. At-Bo, Atdabanian to Botoman; To-At, Tommotian to Atdabanian.

	Aldan	Byd'yangaya	Churan	Oy- Muran (To-At)	Oy- Muran (At-Bo)	Titirikteekh	Zhurinskiy Mys'
Aldan	—	0.0301	0.0863	<b>0.00017</b>	<b>0.00376</b>	<b>0.00406</b>	<b>0.00816</b>
Byd'yangaya	0.415	—	0.535	<b>0.0103</b>	0.191	0.0974	0.303
Churan	0.486	0.263	—	0.0633	0.510	0.582	0.414
Oy-Muran (To-At)	0.661	0.351	0.450	—	0.290	0.0668	0.115
Oy- Muran (At-Bo)	0.525	0.219	0.275	0.225	—	0.213	0.708
Titirikteekh	0.493	0.217	0.249	0.266	0.204	—	0.603
Zhurinskiy Mys'	0.500	0.204	0.300	0.282	0.157	0.153	—

### Comparisons of the Distribution of Mean Outer-Wall Pore Sizes between Localities

The sample size of mean pore sizes calculated for each locality were: Aldan = 14, Byd'yangaya Creek = 54, Churan = 10, To-At Oy-Muran = 32, At-Bo Oy-Muran = 40, Titirikteekh = 71, and Zhurinskiy Mys' = 35. The results for the two sample Kolmogorov-Smirnov tests are shown in the Table 2. A majority of the significant results involve Aldan, suggesting that the distribution at this locality is particularly distinct. Byd'yangaya Creek and To-At Oy-Muran also had significantly different distributions. Aldan and Byd'yangaya Creek have smaller mean and median pore sizes than other localities (Table 3), and To-At Oy-Muran contains relatively higher numbers of specimens with large mean pore sizes. The other localities generally have distributions between these extremes.

### Discussion of Method Validity

#### Analyses of Transverse and Longitudinal Measurements from the Same Specimens

The results support the hypothesis that the two methods are measuring the same pore diameter and that both methods for taking measurements give a similar approximation of the mean pore size of a specimen. This

supports the validity of measuring a specimen's pore size with one method when only one view is available. A consequence of studying fossil material from extinct organisms is the difficulty of investigating any further whether the mean pore size estimated by the two methods is in fact the true restrictive width. However, this uncertainty is minimized by the close agreement of the two methods, which were both logically devised to measure the pore diameter at the narrowest point. The methodology will allow for the rapid and reliable measurement of the restrictive pore size of specimens for which only one view is available.

There are two possible causes of the variability of the measurements used to calculate the mean pore size for each specimen. One is that the variation in measurement reflects true natural variation in the pore size of a specimen. The rest of the variation would be due to measurement error, which could be caused by inaccurately measuring the diameter at the narrowest point of the pore: this is thought to have had minor effect, as the equipment used was well calibrated and measured with high precision (calculated as being correct within 0.4–2 µm over the measurement range of 25–273 µm, thereby representing an error range of

TABLE 3. Mean and median outer-wall pore sizes for the archaeocyaths measured at each locality. At-Bo, Atdabanian to Botoman; To-At, Tommotian to Atdabanian.

	Aldan	Byd'yangaya	Churan	Oy-Muran (To-At)	Oy-Muran (At-Bo)	Titirikteekh	Zhurinskiy Mys'
Median	52.3	62.9	63.6	90.9	75.9	72.2	72.3
Mean	53.0	70.3	85.1	102.4	89.0	79.8	84.9



0.7–1.6%). The other component of measurement error was the measuring of pores at a point that was not exactly the “true” narrowest point of the pore. As explained in the “Materials and Methods” section, this could lead to either under- or overestimation of pore size depending on the cut of the section; this is difficult to quantify but was controlled for through examination of pores from multiple orientations and comparative analysis of longitudinal and transverse cuts. The proportion of the variability attributable to these factors cannot be calculated from the data. Regardless of the cause, the results of the correlation and regression analysis suggest the impact of these factors on the study is relatively minor. Analyses suggested that standard deviation increased with mean pore size, and so the overall measurement error and/or natural variability within a specimen is thought to have increased with mean pore size: either of these explanations are plausible. The effect of the increase in the variation of measurements on mean pore size calculations was reduced, because the mean pore size for a specimen was based on measurements taken from multiple pores. The results showed no evidence of the variability in measurements being different for either method, so the measurement error is the same for both methods. This suggests that both methods are equally reliable for measuring pore size. On this basis neither method can be recommended over the other.

#### Analyses of Transverse and Longitudinal Measurements when Only One Type of Outer-Wall Pore View Was Taken per Specimen

The unexpected trend for longitudinal measurements to be lower than transverse measurements in specimens with only one type of pore cross section may be best explained by sampling bias. Longitudinal measurements may tend to be taken from specimens with smaller pore sizes, because large pores viewed in longitudinal section are more likely to appear incomplete, as you do not see a definite margin in this view, just a space in the wall, which when very large may be interpreted as dissolution or fracture of the wall. As a result, longitudinal measurements were less suitable for inclusion in

the study. This bias would explain the significant result of the *t*-test. Until the causes of this trend are resolved, the effect it has on the data is unknown, although if the explanation suggested is correct, it is likely that specimens with larger pores will be underrepresented. The effect of this should be relatively small, because only 16.4% of the specimens had only longitudinal pores. If a bias is found for longitudinal measurements, future studies may consider not including them. There is no evidence at the moment to suggest that these biases were present, however.

The difference between the means of longitudinal and transverse pores could also reflect the measurement methods of the smallest of the minimum measures for longitudinally viewed pores and the largest of the minimum measures for transversely viewed pores. This is interesting, because when the data from specimens in which both pore types could be measured are taken together, no significant difference could be found. This suggests that the overestimation of the mean from transverse pores alone could be being balanced out by the underestimation of the mean from the longitudinal pores alone. However, it is worth noting that these measures are still based on real pores, and it is only the mean that is affected, not the overall maximum. By performing our subsequent analyses with the means of the data and not the upper range value of maximum diameter for estimating prey size, we are taking a conservative approach to prey size range, as a given archaeocyath may have had some larger pores than the mean pore size for the specimen.

#### Quantifying the Effect of Living Tissue on Restrictive Pore Size

The restrictive pore size in life would have been constricted by the presence of the living cells that cover the body of sponges. In the closest living modern analogue to archaeocyaths, *Vaceletia*, the thickness of live cells covering the body wall is estimated to be between 2 and 20  $\mu\text{m}$  (Kruse 1990). This comports well with direct evidence from fossil archaeocyaths, which suggests that the cellular layer is of a similar scale (see Kruse 1990: Fig. 6). The outer-wall pore diameter is constricted, therefore, by 4 to 40  $\mu\text{m}$  (see Figure 9A), as the pore has living

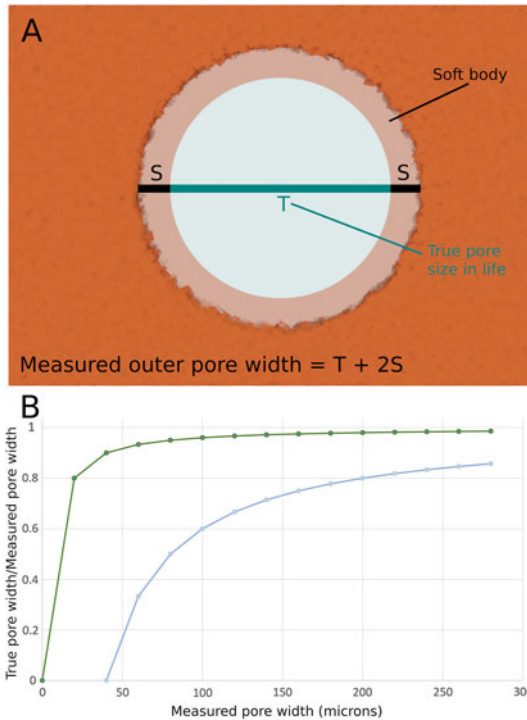


FIGURE 9. A, Schematic representation of the lining of the mineralized archaeocyath body wall with living cells. These cells would restrict the open pore size. B, Plot to show the percentile effects of the estimated cell thickness on the outer-wall pore diameter. The two curves show the maximum possible cell thickness (40 μm—lower curve, as it has a great effect on open pore diameter) and minimum possible cell thickness (4 μm—upper curve, as it has a lesser effect on open pore diameter).

tissue around the entire circumference and constricts both margins of the diameter. The effects of this constriction on the present analysis is, however, insignificant, as the error can be well constrained and becomes insignificant as the pores get larger (Figure 9B). This could suggest a potentially hugely significant error on the smallest of the specimens, as the minimum outer-wall pores were ca. 25 μm, thus, in extremis, the entire pore could be covered by living cells (max. 40 μm), rendering the pore useless for suspension feeding. This implies the smallest pores had a cellular covering toward the thinner range of the spectrum. The minimum cell coverage (4 μm) on the smallest outer-wall pores measured reduces our smallest pores to ca. 21 μm, making little difference when we are considering their likely prey. However, by the time we are considering the

largest pores, the error is constrained between a negligible 1.45% (for 4 μm out of 273 μm) to a manageable 14.5% (40 μm out of 273 μm). Thus, when considering the maximum size of prey that could be consumed by the largest pores (273 μm) measured in our study, we can constrain these pores to between 233 and 269 μm when allowance is made for the cells covering the archaeocyath in life. These ranges are significant when one examines the size ranges of possible prey groups, as we consider in the following section.

### Discussion of Implications for Cambrian Ecology

The data collected on outer-wall pore diameters provide information on the maximum size of plankton that could enter into the interval to be phagocytized by the archaeocyath. This study focused on only a few sites and a few genera, namely: *Nochorocyathus*, *Coscinocyathus*, *Rotundocyathus*, *Erismacoscinus*, and *Tumuliolyntus* (Fig. 3). As archaeocyaths are a diverse group with a great deal of disparity in their skeletal morphology, these taxa do not represent the global range that could be found for archaeocyathan pores. It is therefore possible that the distribution of pore sizes could be different with a different sample of taxa, at different localities, and in different paleoenvironments. It is possible that other taxa could extend the range of pore sizes both upward and downward. Our conclusions are therefore conservative when considering total group Archaeocyatha.

How archaeocyaths fed has been the source of some debate. It has been suggested that archaeocyaths could possibly have housed symbiotic photoautotrophs that provided nutrition for the sponge (Wood 1999; Debrenne 2007). However, a photosymbiotic mode of life is now considered unlikely for a number of reasons. First, many archaeocyaths lived in areas of high sediment input, with high seston input, particularly of mud-sized particles (Kruse et al. 1995; Debrenne 2007). As a result, light penetration would have been very poor, even in the most shallow-water environments that archaeocyaths inhabited; this would have made photosymbiosis unreliable and low

yield. Second, carbon isotope data do not show the fractionations between archaeocyaths and marine cements that would be expected if the archaeocyaths were photosynthetic; this has been replicated at different sites in Australia (Surge et al. 1997) and those sites in this study from Siberia (Brasier et al. 1994). Finally, it has been argued that archaeocyaths predominantly lived in nutrient-rich environments, because they are often found co-occurring with fossil organisms with shells made with the bio-limiting nutrient phosphorous as an important component (Brasier 1991; Surge et al. 1997). While such eutrophic conditions are very good for photosynthetic organisms, such as plants and free-living algae, it is very unusual to find animal–algal photosymbioses in such conditions, with modern reefal associations of this type strongly correlated with nutrient-poor conditions (Surge et al. 1997; Gili and Coma 1998; Kiessling 2009). As a result, it is generally thought that bacterioplankton made up the main food resource for archaeocyaths (Wood et al. 1993; Kruse et al. 1995; Debrenne and Zhuravlev 1997). This is based on comparisons with studies of modern sponge ecology that show bacteria form a substantial part of many modern sponge diets (Reiswig 1971; Leys and Eerkes-Medrano 2006), with bacterioplankton generally falling in the 0.2–2  $\mu\text{m}$  range (see Fig. 10). Outer-wall pores in modern sponges are typically in the 30–60  $\mu\text{m}$  range and can commonly reach 200  $\mu\text{m}$  (Bergquist 1978). However, the digestion of cells takes place in the aquiferous system in specialized choanocyte chambers, and the entrances to the choanocyte chambers are typically 5–10  $\mu\text{m}$  (Bergquist 1978; Bannister et al. 2012); thus, only particles smaller than 10  $\mu\text{m}$  can be digested by most modern sponges. Particles between 10 and 100  $\mu\text{m}$  can enter the sponge and travel through the aquiferous system but cannot enter the choanocyte chambers (Bannister et al. 2012), while particles larger than 100  $\mu\text{m}$  have very little chance of entering the body of most modern sponges. The body size of archaeocyaths was significantly smaller on average than that of modern sponges (averages of 10.6 mm vs. 94.1 mm were found according to Cordie and Dornbos [2019]), yet our analysis indicates comparable outer-wall

pore sizes in archaeocyaths and modern sponges. However, the internal morphology of archaeocyaths was quite unlike that of modern sponges. In archaeocyaths, digestion took place in the intervallum between the inner and outer wall—essentially this is equivalent of the choanocyte chambers in modern sponges. The entrance to the intervallum was through the outer-wall pores and there were no additional skeletal constrictions. The prey size and particle size were therefore not differentiated by the internal skeletal anatomy in archaeocyaths as they are in modern sponges. As pores in archaeocyaths are consistently two orders of magnitude larger than the size of bacteria, this could have made them susceptible to having to deal with higher levels of sediment input (Bell et al. 2015), which is highly problematic for sponges (Bannister et al. 2012), than would be necessary if archaeocyaths had much smaller pores. As a result, there needs to be consideration of whether larger plankton were an important part of the archaeocyath diet.

Even considering the fact that pores may have been slightly restricted by living matter, all of the archaeocyath pores measured were well over 20  $\mu\text{m}$  in diameter. This indicates that the whole size range of nanoplankton (2–20  $\mu\text{m}$ ) as well as a proportion of microplankton (20–200  $\mu\text{m}$ ) could easily enter the intervallum (Fig. 10; Sieburth et al. 1978; Omori and Ikeda 1984). Generally, studies agree that phytoplankton in the nano- and microplankton size range form a significant part of the diet in most modern sponges (see review by Riisgård and Larsen 2010). These larger plankton (nano and micro) are believed to be taken up by cells such as the amoebocytes and collenocytes that line the inhalant passages (Conover 1981; Riisgård and Larsen 2010). Plankton larger than 5  $\mu\text{m}$  formed ~15% of the ingested carbon of the demosponge *Dysidea avara*, but a capacity for ingesting a broad range of food particles, particularly phytoplankton, was important for sustaining a constant food supply during winter when nutrient flux was lower (Ribes et al. 1999). These studies support the hypothesis that nanoplankton and microplankton may have formed an important part of the archaeocyath diet.



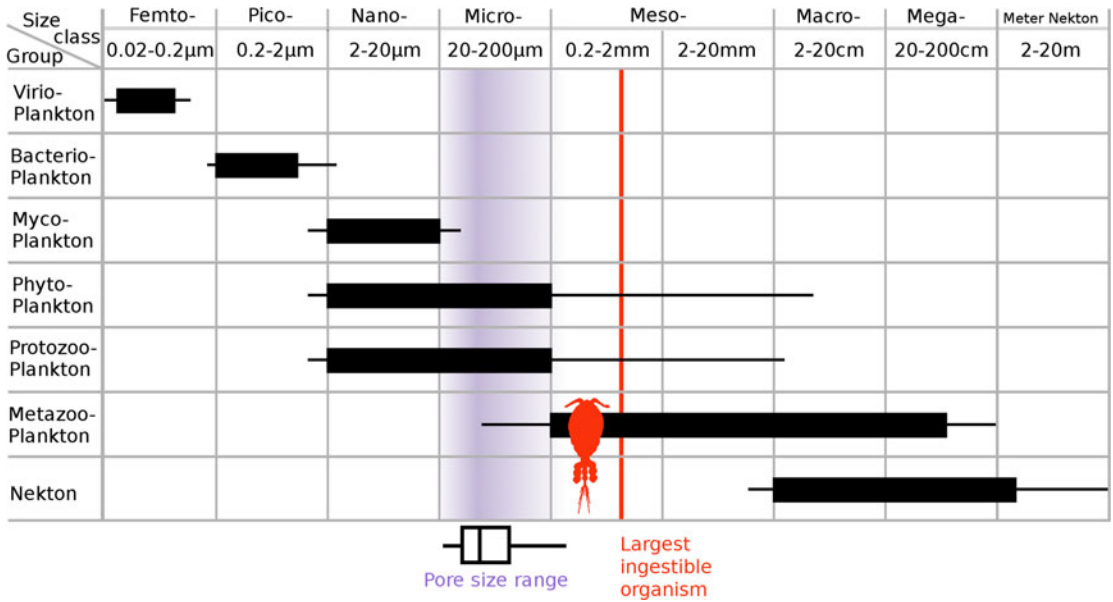


FIGURE 10. Relationship between the size classification of plankton and the biological function/phylogenetic class of plankton (after Sieburth and Smetacek 1978); note that horizontal scale is logarithmic. Phytoplankton consists of photosynthetic single-celled eukaryotic plankton and all autotrophic and mixotrophic single-celled eukaryotic plankton. Protozooplankton includes all single-celled heterotrophic eukaryotes, such as the ciliates and amoeboids. Metazooplankton includes all metazoan heterotrophic plankton and juvenile planktonic metazoans. The light gray (purple outline) shading indicates the density of the data of archaeocyath mean pore sizes. The vertical line indicates the theoretical maximum length of plankton that could be consumed by the largest restrictive pores found in this study. Based on a typical 3:1 length to width ratio for copepods (Fernandez Araoz 1991) and micro-current alignment of nonspherical prey items (Visser and Jonsen 2000), a maximum prey body size would be  $3 \times 269 \mu\text{m} = 807 \mu\text{m}$ . Rather than simply being capable of eating bacterioplankton in the picoplankton range, even the smallest-pored archaeocyath would have been able to consume the nanoplankton range of the single-celled eukaryotic plankton groups, with several of the archaeocyaths being able to carnivorously consume micrometazoans.

Nanoplankton and microplankton size classes can be produced by an array of different organisms (as can be seen from Fig. 10, following Sieburth et al. [1978]). Indeed, the 2–200  $\mu\text{m}$  range is the only major class of plankton size that is commonly produced by a number different major types of organism (e.g., the picoplankton at 0.2–2  $\mu\text{m}$  size range are produced almost exclusively by bacteria; the megaplankton at 20–200 cm are exclusively animal). Microplankton, however, are commonly produced by fungi (mycoplankton), photosynthetic eukaryotes (phytoplankton), and heterotrophic eukaryotes (protozooplankton). Using the restrictive pore size data to make predictions of which specific nanoplankton and microplankton were potentially being consumed by these archaeocyaths is complicated by the fact that the planktonic assemblages before the great Ordovician biodiversification event are believed to have been quite different

from present-day assemblages, and very little is known about them (Servais et al. 2010). Known Cambrian phytoplankton are generally classified as acritarchs (see review by Servais et al. 2010), a polyphyletic group that includes any organic walled microfossil of uncertain phylogenetic affiliation (Evitt 1963), with sizes on the scale of tens to low hundreds of micrometers (Butterfield 1997). This is the scale at which restrictive pore sizes would start to have had an effect on which plankton could enter an archaeocyath for these approximately spherical prey items. The fossilized remains of acritarchs around the Siberian bioherm localities (Kruse et al. 1995) suggest it is likely that these organisms would have been available as an archaeocyath food source.

Our results also suggest that archaeocyaths were able to consume Eumetazoa. The archaeocyath restrictive pore size range in our study extends to a maximum of 273  $\mu\text{m}$  (max. 233–

269  $\mu\text{m}$  when considering the soft-tissue range), which is well into the range of eumetazoan zooplankton (metazooplankton in Fig. 10). Further, the restrictive pore size measured on the archaeocyath only needs to be the size of the smallest physical dimension of the object consumed (i.e., width), not the largest dimension (i.e., length), if the prey items are not spherical. There is substantial evidence to suggest that feeding currents cause the reorientation of non-spherical prey objects to align the smallest dimension perpendicular to the current direction, allowing the consumption of much larger particles (Visser and Jonsson 2000). Metazooplankton can be as small as 50  $\mu\text{m}$  in length, and in particular, larval stages fall well within the microplankton size class and could uncontroversially have been consumed by an archaeocyath. Metazooplankton that act as secondary consumers, such as copepods, are commonly found at around 600  $\mu\text{m}$  in length (in the mesoplankton size class), and typically have a length to width ratio of around 3 to 1 (Fernandez Araoz 1991). This would mean that, with a short axis size of around 200  $\mu\text{m}$ , they could also be consumed by archaeocyaths at the larger end of the pore size spectrum when aligned by feeding currents. The largest pores found in our sample would allow consumption of copepods of a size up to ca. 800  $\mu\text{m}$  in length, given current alignment. This suggests that archaeocyaths could have been carnivorous, similar to many other modern sponges (Vacelet and Boury-Esnault 1995; Vacelet 2006). Most sponges that are carnivorous capture small crustaceans such as copepods (Vacelet and Boury-Esnault 1995) and do so in nutrient-poor areas of the ocean where macrophagy becomes more energetically efficient than filter feeding microscopic particles (Gili and Coma 1998). Ingesting such energetically difficult large prey items would likely necessitate a slower processing time by the archaeocyath. Studies of the ingestion of isotope-tagged prey in modern sponges suggests that prey can be retained inside the sponge for a period of up to 2 weeks, providing considerable time averaging of isotope fractionations with the sponge body itself (Kahn et al. 2018). It is clear that sponges can take extensive amounts of time to process food items. It is highly likely that the

intervallum space in the archaeocyath (see Fig. 1A) is where the ingestion of food took place (Debrenne et al. 2012). It is possible that micro- and mesoplankton could have entered this area, become trapped, and then remained there as the sponge slowly digested them. Microscopic phosphatized fossils of “Orsten-type” fossils provide the earliest evidence of planktonic metazoan larvae (Daley et al. 2018). These fossils are three-dimensionally replicated in phosphate and are widespread both temporally and geographically (Maas et al. 2006). Taxa such as *Yicaris dianensis* and *Wujicaris muelleri* from the phosphatic Yu’an-shan Formation, China (Zhang et al. 2007, 2010), are at least 514 Myr old (Wolfe et al. 2016) and are directly comparable to larvae of well-studied arthropods (Zhang et al. 2010). At an age of around 514 Ma these fossils are only slightly younger than most of the archaeocyaths that comprise the present study (ca. 520 Ma; see Fig. 2), and coeval with the youngest specimens herein (Atdabanian Series 2, Stage 3). Such prey would have been available to archaeocyaths.

The analysis also shows that there is significant variation in the distribution of outer-wall pore sizes between some of the localities. All of the restrictive pore sizes were within the microplankton range, but some archaeocyathan assemblages had significantly larger restrictive pore sizes, and thus could have consumed larger microplankton. Specimens from Aldan and Byd’yan-gaya have significantly smaller restrictive pore sizes than the other localities, meaning these archaeocyaths had a narrower range of possible prey items and a smaller upper limit on prey size. The specimens measured from To-At Oy-Muran had significantly larger restrictive pore sizes and so would have had the potential to take up a greater proportion of larger microplankton, and potentially mesoplankton.

Regional variations in fossil compositions are commonly attributed to a combination of ecological, environmental, and taphonomic factors (Zhao et al. 2012). Taphonomic explanations probably have a limited role in causing pore size variation, because archaeocyath pores are usually well preserved. Outer-wall pore size variation is more likely the result of differing compositions of planktonic communities at

different localities, with archaeocyaths at each having adapted to extract the range of plankton sizes that were found in higher abundance. It could also be that species with larger pores could potentially have fed on a wider variety of plankton, lending flexibility to their feeding mode, which would be advantageous in many situations, for instance, during seasonal variations in food abundance. In bioherms where there was more intense competition for the food resource, variations in pore sizes could allow resource partitioning in the archaeocyaths. Other factors could alter local archaeocyathan community composition, not least of which were their many other morphological characters that were also subject to selection. The present study shows that outer-wall pore size differences are statistically significant between sites and that this character is therefore one worthy of consideration when exploring ecological and evolutionary scenarios, but this does not preclude other factors also being significant.

Prey partitioning allows many species to form a single assemblage in a given location without increasing competition to unsustainable levels at which the assemblage would disintegrate. Thus, a high-diversity system can be established and maintained in one hydrodynamic regime (Lesser et al. 1994). This is most readily achieved by limiting the range of prey size choice. Organisms that ingest small particles and require higher flow rates can then live in the same place as organisms that ingest larger particles and can tolerate much lower flow rates (but will happily live in areas of high flow rate [Gili and Coma 1998]). Active suspension feeders that generate currents to bring prey toward themselves are more energetically efficient at eating small prey, and sponges are remarkably efficient at this, expending only 0.8% of respiratory energy on pumping (Riisgaard and Larsen 1995). So changes in prey size, though effecting this efficiency, are not critical to the ability to survive in a particular hydrodynamic regime, as the filtration system in sponges is so energetically efficient. In modern oceans, sponges dominate deep-sea filtration, but cnidarian reefs dominate in shallow temperate seas (Gili and Coma 1998). This is not the case in the Cambrian, when there were no coral-dominated reefs (not

until the Tabulate coral reefs of the Ordovician; see Landing et al. 2018) and when archaeocyathan reefs dominated the shallow-marine successions in epicontinental seas from temperate to tropical waters (Gandin and Debrenne 2010). It is therefore quite possible that archaeocyaths functioned more like modern coral reefs than like modern sponge reefs. In this sense, they would have dominated the energy flow from the pelagic to benthic systems in Cambrian seas.

The variation in the average upper bound of the size of plankton archaeocyaths could take up could also have been influenced by other factors. For example, bracts (see Fig. 5C), which reduce the size of food particle that could enter the archaeocyath, are proposed to be an adaptation to environmental factors such as locally high water turbulence (Debrenne et al. 2012). This could mean that variation in pore size distributions reflects variation in water turbulence between the localities. Water turbulence, flow rate, and seston concentration are all crucial factors that affect how efficiently filter feeders can take up prey (Gili and Coma 1998); however, they are all connected to prey selection and are themselves not mutually exclusive factors. Bioherms at the Siberian localities are split into domains, each of which would have had a different microclimate (Kruse et al. 1995). The fossil sites examined can be divided into two main groups based on field observations (Kruse et al. 1995; Rozanov et al. 2008; Gandin and Debrenne 2010). The first of these is a lower-diversity and lower-energy grouping of Aldan + Byd'yangaya + Churan, characterized by high proportions of the encrusting calcimicrobe *Renalcis* (James and Gravestock 1990), lower levels of mud input, and small archaeocyaths that are mainly of the stick and bowl type. The second type is a higher-diversity and higher-energy grouping of Oy-Muran + Titirikteekh + Zhurinskiy Mys', characterized by a lower proportion of *Renalcis*, high levels of mud input, and a full array of archaeocyath types, including large stick archaeocyaths and large ramose archaeocyaths, as well as the smaller types found elsewhere (Kruse et al. 1995). This fits well with the data from the pairwise mean pore sizes between sites, which indicated that Aldan and Byd'yangaya and Churan were statistically similar, but



Aldan was significantly different from all the other sites, while high levels of support were also found for distinguishing Byd'yangaya from the To-At Oy-Muran. The highly erect and ramose forms found at Oy-Muran, Titirikteekh, and Zhurinskiy Mys', alongside a much higher diversity, suggest these sites had much higher water flow rates and higher seston concentrations, which sustained the more complex forms and thereby allowed the development of much greater taxon heterogeneity. This suggests that at these three higher-energy sites, the sponge/*Renalcis* reef was functioning much more like a modern highly heterogeneous community (such a tropical coral-algal system) than a low-diversity system such as a deep-water sponge community. These reefs, particularly those found on the transition zone between shallow and deep water (Gili and Coma 1998), as is the case for the Siberian archaeocyathan reef (Kruse et al. 1995; Rozanov et al. 2008), are maintained by extensive prey partitioning. This takes place across a broad range of prey sizes from picoplankton to mesoplankton, with prey ranging from bacteria to metazoan plankton. These highly structured communities are also associated with highly structured and diverse plankton, and this was likely the case for the Siberian reefs of the lower Cambrian. This indicates that the planktonic system was well developed by the Tommotian stage (ca. 525–521 Ma), with ecosystem construction well underway by this time. Archaeocyathan reefs were a critical locus for sustaining and expanding biodiversity, just like modern coral barrier reefs. The central and essential role that archaeocyathan reefs must have therefore played in the Cambrian explosion and the accelerating metazoan ecological expansion can hardly be overstated.

### Conclusions

This study has developed, tested, and applied a new methodology for investigating the feeding ecology of archaeocyaths. By following the specific methods recommended here, restrictive outer-wall pore size data can be measured quickly and easily from pores preserved in both transverse and longitudinal

sections. Archaeocyath skeletons are regularly preserved with their pores intact, and our method provides a novel means of gathering ecologically useful information from these extinct sponges. Statistical analyses of restrictive pore size data identified differences between Siberian localities, implicating prey partitioning as a likely cause. The study also provides evidence that nanoplankton, microplankton, and mesoplankton could have made up some proportion of the archaeocyath diet, in contrast to previous assumptions that they were bacteriophages. As sponges provide a critical link in marine ecosystems connecting the energy contained in the plankton to the benthos (Gili and Coma 1998), it is essential to understand the role archaeocyaths played in the early Cambrian oceans. As the first metazoan-dominated ecosystems were constructed during the Cambrian explosion, the roles of prey partitioning and intraspecific competition can now be understood during the construction of the first complex reef ecosystems. Further, while the Archaeocyatha are confined to the Cambrian Period they are not the only group of sponges to have adopted such a peculiar mode of construction (Senowbari-Daryan and García-Bellido 2002; Debrenne et al. 2012; Antcliffe et al. 2014). This raises the prospect that other sponges that possessed large chambers and large pores (often >1 mm), and therefore could have ingested zooplankton, may have been more ecologically complex. These sphinctozoan forms are hugely abundant and diverse, reaching an acme in the Permo-Triassic before becoming almost extinct at the end-Cretaceous extinction (Senowbari-Daryan and García-Bellido 2002). While they have meaningful morphological differences in comparison to archaeocyaths, they could still be prey fractionating using their pores. This methodology could therefore be of broad applicability to understanding the sponge contribution to reef dynamics through much of the Phanerozoic.

### Authors' Contributions

J.B.A. and A.C.D. designed the research. W.J. collected data in the collection of the MNHN (Paris, France) and performed initial statistics under the guidance of J.B.A. and A.C.D.

J.B.A. performed further statistical tests and reran all statistics for robustness. W.J. photographed specimens. J.B.A. made all the figures and plates. W.J. helped to draft the article. J.B.A. was the primary writer. J.B.A. and A.C.D. developed and wrote the “Discussion” and “Conclusion” sections.

### Acknowledgments

The authors would like to thank G. Taylor (Zoology, Oxford) and P. Kruse (South Australia Museum) for their advice and helpful discussions. A. Kerner (MNHN, Paris) organized access to the fossils and helped to identify specimens. F. Debrenne (MNHN, Paris) is thanked for her extraordinary contribution to this field and for her help and encouragement over many years. W.J. acknowledges funding from Jesus College (Oxford University), an Allison R. “Pete” Palmer Award from the Palaeontological Society, and the Palaeontological Association (grant reference: PA-UB201502). A.C.D. and J.B.A. acknowledge funding from the Oxford University Museum of Natural History and the support of the University of Lausanne, Switzerland.

### Literature Cited

- Antcliffe, J. B. 2013. Questioning the evidence of organic compounds called sponge biomarkers. *Palaeontology* 56:917–925.
- Antcliffe, J. B. 2015. The oldest compelling evidence for sponges is still early Cambrian in age—reply to Love and Summons (2015). *Palaeontology* 58:1137–1139.
- Antcliffe, J. B., R. H. Callow, and M. D. Brasier. 2014. Giving the early fossil record of sponges a squeeze. *Biological Reviews* 89:972–1004.
- Balsam, W. L., and S. Vogel. 1973. Water movement in archaeocyathids: evidence and implications of passive flow in models. *Journal of Paleontology* 47:979–984.
- Bannister, R., C. Battershill, and R. De Nys. 2012. Suspended sediment grain size and mineralogy across the continental shelf of the Great Barrier Reef: impacts on the physiology of a coral reef sponge. *Continental Shelf Research* 32:86–95.
- Bell, J. J., E. McGrath, A. Biggerstaff, T. Bates, H. Bennett, J. Marlow, and M. Shaffer. 2015. Sediment impacts on marine sponges. *Marine Pollution Bulletin* 94(1–2):5–13.
- Bergquist, P. R. 1978. *Sponges*. University of California Press, Berkeley.
- Brasier, M. 1976. Early Cambrian intergrowths of archaeocyathids, *Renalcis*, and pseudostromatolites from South Australia. *Palaeontology* 19:223–245.
- Brasier, M. 1991. Nutrient flux and the evolutionary explosion across the Precambrian–Cambrian boundary interval. *Historical Biology* 5(2–4):85–93.
- Brasier, M. D., R. M. Corfield, L. A. Derry, A. Y. Rozanov, and A. Y. Zhuravlev. 1994. Multiple Delta-13c excursions spanning the Cambrian explosion to the Botomian crisis in Siberia. *Geology* 22:455–458.
- Butterfield, N. J. 1997. Plankton ecology and the Proterozoic–Phanerozoic transition. *Paleobiology* 23:247–262.
- Carrera, M. G., and J. P. Botting. 2008. Evolutionary history of Cambrian spiculate sponges: implications for the Cambrian evolutionary fauna. *Palaios* 23:124–138.
- Conover, R. J. 1981. Nutritional strategies for feeding on small suspended particles. Pp. 363–395 in A. R. Longhurst, ed. *Analysis of Marine Ecosystems*. Academic, New York.
- Cordie, D. R., and S. Q. Dornbos. 2019. Restricted morphospace occupancy of early Cambrian reef-building archaeocyaths. *Paleobiology* 45:331–346.
- Cordie, D. R., S. Q. Dornbos, P. J. Marenco, T. Oji, and S. Gonchigdorj. 2019. Depauperate skeletonized reef-dwelling fauna of the early Cambrian: insights from archaeocyathan reef ecosystems of western Mongolia. *Palaeogeography, Palaeoclimatology, Palaeoecology* 514:206–221.
- Daley, A. C., J. B. Antcliffe, H. B. Drage, and S. Pates. 2018. Early fossil record of Euarthropoda and the Cambrian explosion. *Proceedings of the National Academy of Sciences USA* 115:5323–5331.
- Debrenne, F. 2007. Lower Cambrian archaeocyathan bioconstructions. *Comptes Rendus Palevol* 6(1–2):5–19.
- Debrenne, F., and J. Vacelet. 1984. Archaeocyatha: is the sponge model consistent with their structural organisation? *Palaeontographica Americana* 54:358–369.
- Debrenne, F., and A. Y. Zhuravlev. 1997. Cambrian food web: a brief review. *Geobios* 30:181–188.
- Debrenne, F., A. Y. Zhuravlev, and A. Y. Rozanov. 1989. *Pravil'nye arkhoeotsiaty [Regular archaeocyaths]*. *Trudy Paleontologicheskii Institut Akademiyi Nauk, Moscow*.
- Debrenne, F., A. Y. Zhuravlev, and P. D. Kruse. 2012. Part E (revised), vol. 4, chap. 18: General features of the Archaeocyatha. *Treatise Online* 38:1–102.
- Evitt, W. R. 1963. A discussion and proposals concerning fossil dinoflagellates, hystrichospheres, and acritarchs, II. *Proceedings of the National Academy of Sciences USA* 49:298–302.
- Fernandez Araoz, N. C. 1991. Individual biomass, based on body measures, of copepod species considered as main forage items for fishes of the Argentine shelf. *Oceanologica Acta* 14:575–580.
- Gandin, A., and F. Debrenne. 2010. Distribution of the archaeocyath–calcmicrobial bioconstructions on the Early Cambrian shelves. *Palaeoworld* 19:222–241.
- Gili, J.-M., and R. Coma. 1998. Benthic suspension feeders: their paramount role in littoral marine food webs. *Trends in Ecology and Evolution* 13:316–321.
- Gradstein, F. M., J. G. Ogg, M. Schmitz, and G. Ogg. 2012. *The geologic time scale 2012*. Elsevier, Amsterdam.
- Hammer, Ø., and D. A. Harper. 2008. *Paleontological data analysis*. Wiley, Hoboken, N.J.
- James, N. P., and F. Debrenne. 1980. Lower Cambrian bioherms: pioneer reefs of the Phanerozoic. *Acta Palaeontologica Polonica* 25(3–4):655–668.
- James, N. P., and D. I. Gravestock. 1990. Lower Cambrian shelf and shelf margin buildups, Flinders Ranges, South Australia 1. *Sedimentology* 37:455–480.
- Kahn, A. S., J. W. Chu, and S. P. Leys. 2018. Trophic ecology of glass sponge reefs in the Strait of Georgia, British Columbia. *Scientific Reports* 8:756.
- Khomentovskiy, V., and L. Repina. 1965. The Lower Cambrian of the stratotype section of Siberia. *Institut Geologii i Geofiziki* 14. *Akademia Nauk SSSR Sibirske Otdelenie, Moscow*.
- Kiessling, W. 2009. Geologic and biologic controls on the evolution of reefs. *Annual Review of Ecology, Evolution, and Systematics* 40:173–192.
- Kruse, P. D. 1982. Archaeocyathan biostratigraphy of the Gnalta Group at Mt. Wright, New South Wales. *Palaeontographica Abteilung A* 177:129–212.

- Kruse, P. D. 1990. Are archaeocyaths sponges, or are sponges archaeocyaths. In *The Evolution of a late Precambrian–early Palaeozoic rift complex: the Adelaide Geosyncline*. Geological Society of Australia Special Publication 16:310–323.
- Kruse, P. D., and E. Moreno-Eiris. 2014. Archaeocyaths of the White Point Conglomerate, Kangaroo Island, South Australia. *Alcheringa* 38(1):1–64.
- Kruse, P. D., A. Y. Zhuravlev, and N. P. James. 1995. Primordial metazoan-calcimicrobial reefs: Tommotian (early Cambrian) of the Siberian platform. *Palaios* 10:291–321.
- Landing, E., G. Geyer, M. D. Brasier, and S. A. Bowring. 2013. Cambrian evolutionary radiation: context, correlation, and chronostratigraphy—overcoming deficiencies of the first appearance datum (FAD) concept. *Earth-Science Reviews* 123:133–172.
- Landing, E., J. B. Antcliffe, G. Geyer, A. Kouchinsky, S. S. Bowser, and A. Andreas. 2018. Early evolution of colonial animals (Ediacaran Evolutionary Radiation–Cambrian Evolutionary Radiation–Great Ordovician Biodiversification Interval). *Earth Science Reviews* 178:105–135.
- Lesser, M. P., J. D. Witman, and K. Sebnens. 1994. Effects of flow and seston availability on scope for growth of benthic suspension-feeding invertebrates from the Gulf of Maine. *Biological Bulletin* 187:319–335.
- Leys, S. P., and D. I. Eerkes-Medrano. 2006. Feeding in a calcareous sponge: particle uptake by pseudopodia. *Biological Bulletin* 211:157–171.
- Maas, A., A. Braun, X.-P. Dong, P. C. Donoghue, K. J. Müller, E. Olempska, J. E. Repetski, D. J. Siveter, M. Stein, and D. Waloszek. 2006. The “Orsten”—more than a Cambrian Konservat-Lagerstätte yielding exceptional preservation. *Palaeoworld* 15:266–282.
- McKee, E. H. 1963. Ontogenetic stages of the archaeocyathid *Ethmophyllum whitneyi* Meek. *Journal of Paleontology* 37:287–293.
- Muscente, A., F. M. Michel, J. G. Dale, and S. Xiao. 2015. Assessing the veracity of Precambrian “sponge” fossils using *in situ* nanoscale analytical techniques. *Precambrian Research* 263:142–156.
- Nettersheim, B. J., J. Brocks, A. Schwelm, J. M. Hope, F. Not, M. Lomas, C. Schmidt, R. Schiebel, E. C. M. Nowack, P. De Deckker, J. Pawlowski, S. S. Bowser, I. Bobrovskiy, K. Zonneveld, M. Kucera, M. Stühr, and C. Hallmann. 2019. Putative sponge biomarkers in unicellular Rhizaria question an early rise of animals. *Nature Ecology & Evolution* 3:577–581.
- Omori, M., and T. Ikeda. 1984. *Methods in marine zooplankton ecology*. Wiley, New York.
- Peters, S. E., and R. R. Gaines. 2012. Formation of the “Great Unconformity” as a trigger for the Cambrian explosion. *Nature* 484:363.
- R Core Team. 2018. R: a language and environment for statistical computing. R Foundation for Statistical Computing, Vienna, Austria. <https://www.R-project.org>.
- Reiswig, H. 1973. Population dynamics of three Jamaican Demospongiae. *Bulletin of Marine Science* 23:191–226.
- Reiswig, H. M. 1971. Particle feeding in natural populations of three marine demosponges. *The Biological Bulletin* 141:568–591.
- Ribes, M., R. Coma, and J.-M. Gili. 1999. Natural diet and grazing rate of the temperate sponge *Dysidea avara* (Demospongiae, Dendroceratida) throughout an annual cycle. *Marine Ecology Progress Series* 176:179–190.
- Riisgaard, H. U., and P. S. Larsen. 1995. Filter-feeding in marine macro-invertebrates: pump characteristics, modelling and energy cost. *Biological Reviews* 70:67–106.
- Riisgård, H. U., and P. S. Larsen. 2010. Particle capture mechanisms in suspension-feeding invertebrates. *Marine Ecology Progress Series* 418:255–293.
- Rowland, S. M. 2001. Archaeocyaths—a history of phylogenetic interpretation. *Journal of Paleontology* 75:1065–1078.
- Rowland, S. M., and R. A. Gangloff. 1988. Structure and paleoecology of Lower Cambrian reefs. *Palaios* 3:111–135.
- Rozanov, A. Y., V. Khomentovskiy, Y. Y. Shabanov, G. Karlova, A. Varlamov, V. Luchina, Y. E. Demidenko, P. Y. Parkhaev, I. Korovnikov, and N. Skorlotova. 2008. To the problem of stage subdivision of the Lower Cambrian. *Stratigraphy and Geological Correlation* 16:1–19.
- Savarese, M. 1992. Functional analysis of archaeocyathan skeletal morphology and its paleobiological implications. *Paleobiology* 18:464–480.
- Senowbari-Daryan, B., and D. C. García-Bellido. 2002. Fossil “Sphinctozoa”: chambered sponges (polyphyletic). Pp. 1511–1538 in J. N. A. Hooper, R. W. M. Van Soest, and P. Willenz, eds. *Systema porifera*. Springer, Boston.
- Servais, T., A. W. Owen, D. A. Harper, B. Kröger, and A. Munnecke. 2010. The great Ordovician biodiversification event (GOBE): the palaeoecological dimension. *Palaeogeography, Palaeoclimatology, Palaeoecology* 294:99–119.
- Shea, K., and P. Chesson. 2002. Community ecology theory as a framework for biological invasions. *Trends in Ecology and Evolution* 17:170–176.
- Sieburth, J. M., V. Smetacek, and J. Lenz. 1978. Pelagic ecosystem structure: heterotrophic compartments of the plankton and their relationship to plankton size fractions 1. *Limnology and Oceanography* 23:1256–1263.
- Skorlotova, N. A. 2013. New archaeocyatha from the Atdabanian Stage of the Siberian Platform. *Paleontologicheskii Zhurnal* 47:555–561.
- Surge, D. M., M. Savarese, J. Robert Dodd, and K. C. Lohmann. 1997. Carbon isotopic evidence for photosynthesis in Early Cambrian oceans. *Geology* 25:503–506.
- Vacelet, J. 1977. Une nouvelle relique du Secondaire: un représentant actuel des éponges fossiles Sphinctozoaires. *Comptes rendus de l'Académie des Sciences* 285:509–511.
- Vacelet, J. 2006. New carnivorous sponges (Porifera, Poecilosclerida) collected from manned submersibles in the deep Pacific. *Zoological Journal of the Linnean Society* 148:553–584.
- Vacelet, J., and N. Boury-Esnault. 1995. Carnivorous sponges. *Nature* 373:333–335.
- Visser, A. W., and P. R. Jonsson. 2000. On the reorientation of non-spherical prey particles in a feeding current. *Journal of Plankton Research* 22:761–777.
- Wolfe, J. M., A. C. Daley, D. A. Legg, and G. D. Edgecombe. 2016. Fossil calibrations for the arthropod Tree of Life. *Earth-Science Reviews* 160:43–110.
- Wood, R. 1999. *Reef evolution*. Oxford University Press, New York.
- Wood, R., A. Y. Zhuravlev, and F. Debrenne. 1992. Functional biology and ecology of Archaeocyatha. *Palaios* 7:131–156.
- Wood, R., A. Y. Zhuravlev, and A. Chimed-Tseren. 1993. The ecology of Lower Cambrian buildups from Zuune Arts, Mongolia: implications for early metazoan reef evolution. *Sedimentology* 40:829–858.
- Wörheide, G., and J. Reitner. 1996. “Living fossil” sphinctozoan coralline sponge colonies in shallow water caves of the Osprey Reef (Coral Sea) and the Astrolabe Reefs (Fiji Islands). Pp. 145–148 in J. Reitner, F. Neuweiler, and F. Gunkel, eds. *Global and regional controls on biogenic sedimentation, Vol. 1. Reef evolution. Research reports*. Geologisch-Paläontologisches Institut der Georg-August-Universität, Göttingen, Germany.
- Wulff, J. 2012. Ecological interactions and the distribution, abundance, and diversity of sponges. *Advances in Marine Biology* 61:273–344. Elsevier, Amsterdam.
- Wulff, J. L. 2006. Ecological interactions of marine sponges. *Canadian Journal of Zoology* 84:146–166.
- Zhang, X.-g., D. J. Siveter, D. Waloszek, and A. Maas. 2007. An epipodite-bearing crown-group crustacean from the Lower Cambrian. *Nature* 449:595.



- Zhang, X.-g., A. Maas, J. T. Haug, D. J. Siveter, and D. Waloszek. 2010. A eucrustacean metanauplius from the Lower Cambrian. *Current Biology* 20:1075–1079.
- Zhao, F., S. Hu, J.-B. Caron, M. Zhu, Z. Yin, and M. Lu. 2012. Spatial variation in the diversity and composition of the Lower Cambrian (Series 2, Stage 3) Chengjiang biota, Southwest China. *Palaeogeography, Palaeoclimatology, Palaeoecology* 346:54–65.
- Zhuravlev, A. Y., E. B. Naimark, and R. A. Wood. 2015. Controls on the diversity and structure of earliest metazoan communities: early Cambrian reefs from Siberia. *Earth Science Reviews* 147:18–29.